

Estimating Example Difficulty using Variance of Gradients

Chirag Agarwal ^{*1} Sara Hooker ^{*2}

Abstract

In machine learning, a question of great interest is understanding what examples are challenging for a model to classify. Identifying atypical examples helps inform safe deployment of models, isolates examples that require further human inspection, and provides interpretability into model behavior. In this work, we propose Variance of Gradients (*VOG*) as a proxy metric for detecting outliers in the data distribution. We provide quantitative and qualitative support that *VOG* is a meaningful way to rank data by difficulty and to surface a tractable subset of the most challenging examples for human-in-the-loop auditing. Data points with high *VOG* scores are more difficult for the model to classify and over-index on examples that require memorization.

1. Introduction

Reasoning about model behavior is often easier when presented with a subset of data points that are relatively more difficult for a trained model to learn. This not only aids interpretability through case based reasoning (Kim et al., 2016; Caruana, 2000; Hooker et al., 2019), but can also be used as a mechanism to surface a tractable subset of atypical examples for further human auditing (Leibig et al., 2017; Zhang, 1992), for active learning or to inform model improvements, or to choose not to classify certain examples when the model is uncertain (Bartlett & Wegkamp, 2008; Cortes et al., 2016).

In this work, we start with a simple hypothesis – examples that a model has difficulty learning will exhibit higher variance in gradient updates over the course of training. On the other hand, we expect the backpropagated gradients of the samples that are *relatively easier* to learn will have lower

^{*}Equal contribution ¹University of Illinois at Chicago, Chicago, USA. ²Google Brain, Mountain View, USA. Correspondence to: Chirag Agarwal <chiragagarwall12@gmail.com>, Sara Hooker <shooker@google.com>.

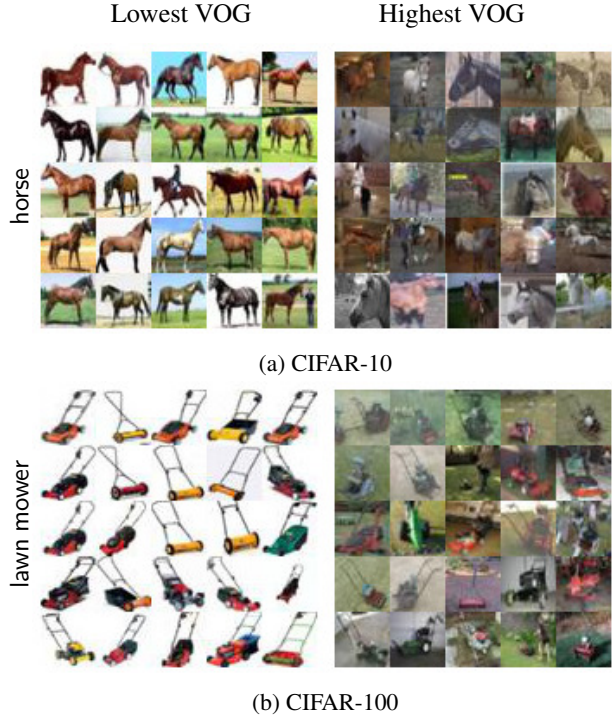


Figure 1. Each 5×5 grid shows the top-25 CIFAR-10 (a) and CIFAR-100 (b) training-set images with the lowest and highest *VOG* scores. Images with lower *VOG* scores appear to over-index on uncluttered backgrounds and prototypical vantage points of the object (standing pose for horse (top) and full view for lawn mower (bottom)), whereas images with higher *VOG* scores tend to feature atypical vantage points and cluttered backgrounds that make the object hard to differentiate.

variance because performance on that example does not consistently dominate the loss over the course of training. The gradient updates for the *relatively easier* examples are expected to stabilize early in training and converge to a narrow range of values.

To explore this hypothesis, we propose class-normalized variance of gradients (which we term *VOG*) as a mechanism of ranking data points by difficulty within a class category and surfacing atypical examples for additional human-in-the-loop auditing. *VOG* computes the variance in input gradients at different intervals in training for each example.

We find that *VOG* identifies clusters of images with clearly

distinct properties (as seen in Fig.1). Low *VOG* scores feature images with far less cluttered backgrounds and more prototypical vantage points of the object relative to images with high *VOG* scores. In contrast, images with high *VOG* scores over-index on images with cluttered backgrounds and atypical vantage points of the object of interest (zoomed in on part of the object, side profile of the object, shot from above). To move beyond anecdotal observations, we seek to quantify whether images with high *VOG* scores are in fact more challenging for the model to classify.

Contributions We present consistent results across two image datasets (Krizhevsky et al., 2009) - CIFAR-10 and CIFAR-100. Our main contributions are:

1. We propose a class-normalized variance gradient score (which we term *VOG*) for determining the relative ease of learning data samples within a given class (Sec. 3.2).
2. We show that *VOG* is an effective tool for ranking the dataset by difficulty. *VOG* assigns higher scores to test-set examples that are more challenging for the model to classify. Restricting evaluation to the test-set examples with the lowest *VOG* greatly improves generalization performance (Sec. 3.3).
3. We use *VOG* to explore how learning differs at different stages of training and show that *VOG* rankings are sensitive to the stage of training. We also investigate whether noisy uninformative examples that require *memorization* will be scored highly by *VOG*. We shuffle the labels of a fraction of the dataset (in a similar experiment to that proposed by (Zhang et al., 2016)) and find that images with shuffled labels have higher *VOG* scores on average than the remainder of the dataset (Sec. 3.3).

Implications of this work It is becoming increasingly important for deep neural networks (DNNs) to make decisions that are interpretable to both researchers and end-users. In sensitive domains such as health care diagnostics (Xie et al., 2019; Gruetzmacher et al., 2018; Badgeley et al., 2019; Oakden-Rayner et al., 2019), self-driving cars (NHTSA, 2017) and hiring (Dastin, 2018; Harwell, 2019) providing tools for domain experts to audit models is of upmost importance. Our work offers an efficient method to rank the global difficulty of examples and surface a possible subset to aid human interpretability. Our results also suggest *VOG* is a successful proxy for identifying samples that are memorized during the training of a deep neural network.

2. Methodology

We consider a supervised classification problem where a DNN is trained to approximate the function F that maps

an input variable X to an output variable Y , formally $F : X \mapsto Y$. Without loss of generality we represent the image input as a feature vector \mathbf{x} . $y \in Y$ is a discrete label vector associated with each input x . Each label y corresponds to one of C categories or classes. A given input image \mathbf{x} can be decomposed into a set of pixels $\{x_i\}_{i=1}^N$. For each image in the training and test set, we compute the gradient of the pre-softmax activation A_n^l with respect to each pixel x_i . Here, l designates the layer of the network and p is the index of the true class probability.

$$\mathbf{S} = \frac{\partial A_p^l}{\partial x_i}$$

This formulation may feel familiar as it is often computed based upon the weights of a trained model and visualized as a image heatmap for interpretability purposes (Baehrens et al., 2010; Simonyan et al., 2013). Here, we instead intend to compute the average variance of the input gradients for the same image across training to arrive at a scalar score.

For $x_i \in x$, we compute the input gradients \mathbf{S}_{ti} at different intervals across training, where t indicates the epoch number. We end up with a set of K gradient snapshots computed at different input steps. We then calculate the mean gradient input over all epochs in training μ_i :

$$\mu_i = \frac{1}{K} \sum_{t=1}^K \mathbf{S}_{ti} \quad (1)$$

For example, if the number of epochs is 300 and the interval between each snapshot is 10, $K = 30$. We note that *VOG* can be computed for both training and test sets by measuring the variance in gradients using checkpoints stored at different points in training. Finally, we compute *VOG* for each data sample:

$$VOG_i = \sqrt{\left(\frac{1}{K} \sum_{t=1}^K \frac{1}{N} (\mathbf{S}_{ti} - \mu_i)^2\right)} \quad (2)$$

Here, N is the total number of pixels in a given image. Hence, for every data sample $x \in X$ we compute a scalar value indicating the variance in gradients score. In order to account for inherent differences in variance between classes, we normalize the *VOG* score by class-level mean and standard deviation. This amounts to asking: *What is the variance of gradients for this image relative to all other exemplars for this class category?*

3. Experimental Evaluations

3.1. Datasets and Training

Datasets: We evaluate our methodology on CIFAR-10 and CIFAR-100 (Krizhevsky et al., 2009).

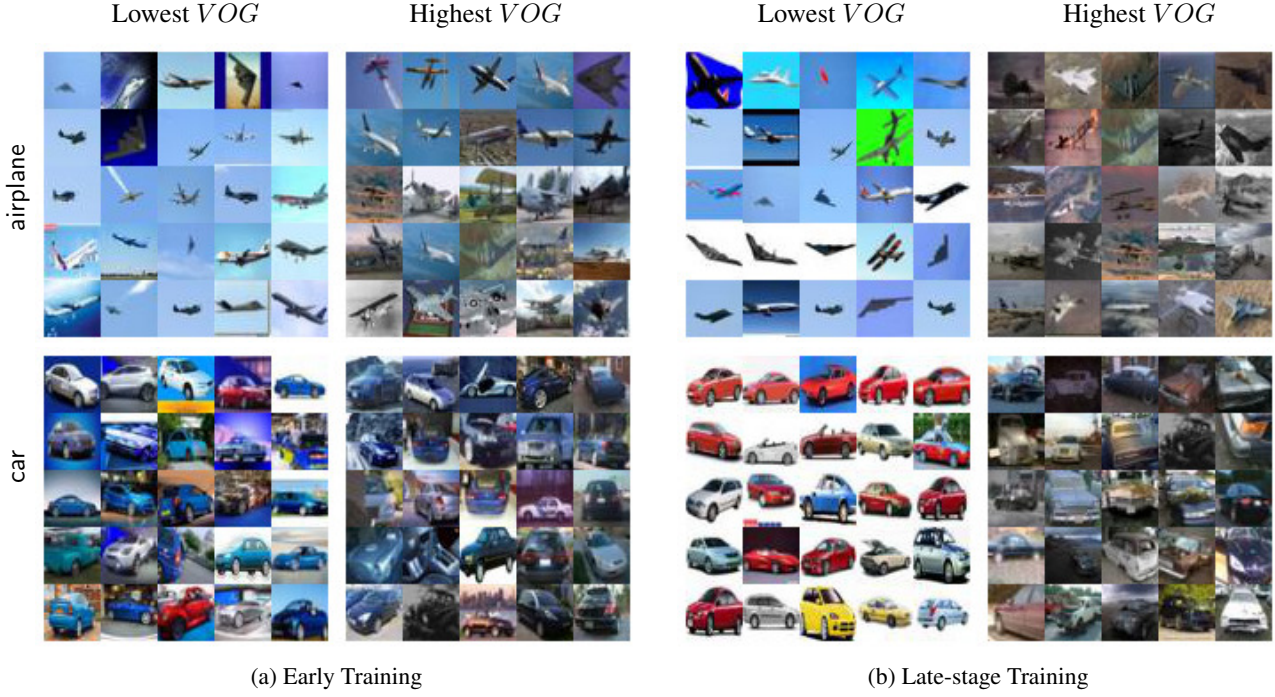


Figure 2. Each 5×5 grid shows the top-25 CIFAR-10 training-set images with the lowest and highest VOG scores in the *Early* (a) and *Late* (b) training stage respectively of two randomly chosen classes. Images with lower VOG scores tend to feature clean backgrounds (blue for airplane (top)), whereas images with higher VOG scores in the *Late* stage are complex with the objects not easily differentiated from the background.

Training: We use a ResNet-18 network (He et al., 2016) for both classification tasks. For each dataset, we train for 350 epochs using stochastic gradient descent (SGD) and compute the input gradients for each sample at the first and last three epochs of the training. We implemented standard data augmentation by applying cropping and horizontal flips of input images. We use a base learning rate schedule of 0.1 and adaptively change to 0.01 at 150th and 0.001 at 250th training epochs.

The model overfitted for both CIFAR-10 and CIFAR-100 datasets with an end training-set and test-set accuracy of 89.57% and 66.86% respectively. We acknowledge this test-set accuracy is not state of the art top-1 performance for these datasets. However, it is suitable for our goal of understanding whether VOG is able to effectively rank examples. It is also necessary to explore the relationship between memorization and VOG scores. For this, we purposefully overfit each model to achieve $\sim 0\%$ training error.

3.2. Relative ranking of image

Across training The first experiment we consider is ranking images based upon the VOG score computed *across training* using gradient snapshots at regularly spaced intervals. For both datasets, we compute gradient snapshots every 10 epochs. We find that VOG computed across training identi-

fies clusters of images with clearly differentiated properties. In Fig. 2, we visualize the 25 images ranked lowest and highest according to VOG . Images with the *lowest VOG* score tend to have uncluttered, often white backgrounds with the object of interest centered clearly in the frame. Images with the *highest VOG* scores have cluttered backgrounds and the object of interest is not easily distinguishable from the background. We also note that images with high VOG score tend to feature atypical vantage points of the objects such as highly zoomed frames, side profiles of the object or shots taken from above.

Early vs late rankings Recent work has shown that there are distinct stages to training in deep neural networks (Achille et al., 2017; Jiang et al., 2020; Mangalam & Prabhu, 2019; Faghri et al., 2020). In our second experiment, we explore whether rankings according to VOG are sensitive to the stage of the training process. Hence, we compute VOG separately for two different stages of the training process, which we term (1) the *Early* stage (first three epochs), and (2) the *Late* stage (last three epochs). Test-set accuracy at the *Early* stage is 44.65% for CIFAR-10 and CIFAR-100 respectively. In the *Late* stage it is 14.16%, and 89.57% and 66.86% for CIFAR-10 and CIFAR-100 respectively.

We find that there is a noticeable visual difference between the image ranking computed for *Early* and *Late* stages of



Figure 3. The 5×5 grid shows the top-25 CIFAR-100 training-set images with the lowest and highest *VOG* scores in the *Early* (a) and *Late* (b) training stage respectively of two randomly chosen classes. Similar to CIFAR-10, lower *VOG* images evidence uncluttered backgrounds (for both apple and boy) in the *Late* training stage. *VOG* also appears to capture a color bias present during the *Early* training stage for both apple and boy (red). The *VOG* images in *Late* training stage present unusual vantage points, with images where the frame is zoomed in on the object of interest.

training. As seen in Fig. 3, for some classes such as boy and apple it appears that *VOG* scores also capture network color bias present during the *Early* training stages. For these classes, the lowest *VOG* scores over-index on boys wearing red shirts and red colored apples.

3.3. Does ranking by *VOG* identify more challenging examples?

A qualitative inspection of examples with high and low *VOG* scores suggests that images with high *VOG* scores are more difficult to classify (as seen in Figs. 2,3). Here, we propose some quantitative experiments to understand whether this is in fact the case.

Test-set error and *VOG* *Is VOG able to effectively discriminate between easy and challenging examples?* We propose an experiment to evaluate the effectiveness of the overall ranking. In Fig. 4, we plot the test-set error of examples bucketed by *VOG* decile. For this and the remainder of the experiments, we compute *VOG* using checkpoints stored from the first and last 3 epochs. Thus, at each point of the x-axis, we are computing the test-set error on the 10% of data whose *VOG* score falls between each decile. Note that we plot error, so lower is better. We show that examples at the lowest percentiles of *VOG* have far lower error

rates. Mis-classification increases with an increase in *VOG* scores. We note that the differences in *VOG* scores across all deciles is more pronounced for CIFAR-100 than CIFAR-10, which may be due to the far more complex number and diversity of categories in CIFAR-100. In contrast, we suspect that there are fewer difficult examples for CIFAR-10 which leads to most examples having low scores with a small subset with high scores and error rates. Additionally, we also observe that the samples in the top-10 percentile category of the *VOG* scores have an higher error rate when compared to the samples in the bottom-10 percentile and the overall testing error rate of the dataset (Fig. 5).

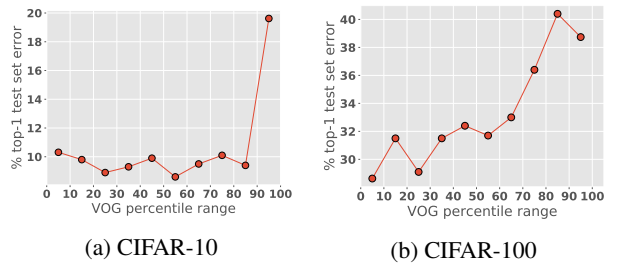


Figure 4. The mean top-1 test set error (y-axis) for the exemplars thresholded by *VOG* score percentile (x-axis). Across both CIFAR-10 and CIFAR-100, we observe that misclassification increases with an increase in *VOG* scores.

Class Level Error Metrics and VOG Here, we explore whether *VOG* is able to capture class level differences in difficulty. We compute *VOG* scores for each image in the test-set of CIFAR-10 and CIFAR-100 (both test-sets have 10,000 images). In Fig. 6, we plot the average absolute *VOG* score for each class against the false negative rate for each class. We find that there is a positive, albeit weak, correlation between the two, classes with higher *VOG* scores have higher mis-classification error rate. The correlation between these metrics is 0.65 and 0.59 for CIFAR-10 and CIFAR-100 respectively. Given that *VOG* is computed a per-example level, we find it interesting that the aggregate average of *VOG* is able to capture class level differences in difficulty.

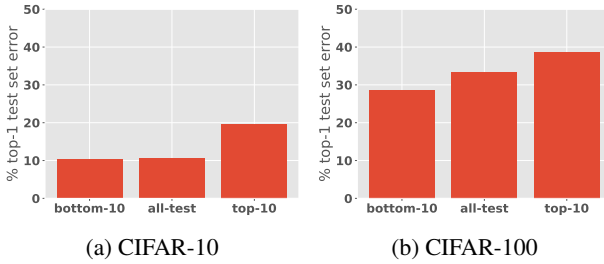


Figure 5. Bar plots showing the mean top-1 error rate (in %) for three group of samples from (1) the subset of the test-set with the bottom 10th percentile of VOG scores, (2) the complete testing dataset, and (3) the subset of the test-set with the top 10th percentile of VOG scores. Across both CIFAR-10 (a) and CIFAR-100 (b) we observe that the group of samples in the top-10 percentile VOG scores have the highest error rate, *i.e.*, contains most number of misclassified samples. For both datasets, model generalization improves on the bottom 10th percentile relative to the entire dataset.

Surfacing examples that require memorization Over-parameterized networks have been shown to achieve zero training error by memorizing examples (Zhang et al., 2016; Feldman, 2020). We explore whether *VOG* is able to identify examples that require memorization and the rest of the dataset. To do this, we replicate the general experiment setup of Zhang et al. (2016) and replace 20% of all labels in the training set with random shuffled labels. We re-train the model from random initialization and compute *VOG* scores at relative intervals *across training* for all examples in the training set. Our network achieves 0% training error which would only be possible given successful memorization of the noisy examples with shuffled labels. *Is VOG able to discriminate between these memorized examples and the rest of the dataset?*

A ranking method that is able to surface memorized examples is a valuable property for an auditing tool because memorized examples are often mislabelled or corrupted which means this subset is a good candidate for further human annotation. To explore this question, in Fig. 7 we

plot the box plot distribution of *VOG* scores for the subset of the data with *shuffled* labels that required memorization beside *correct* labels. We find that the mean and spread of the examples with the shuffled labels are higher when compared to the rest of the dataset. The bar charts are still overlapping for parts of the distribution, but we suspect this to be the case because some of the examples with real labels may also be highly challenging or require memorization.

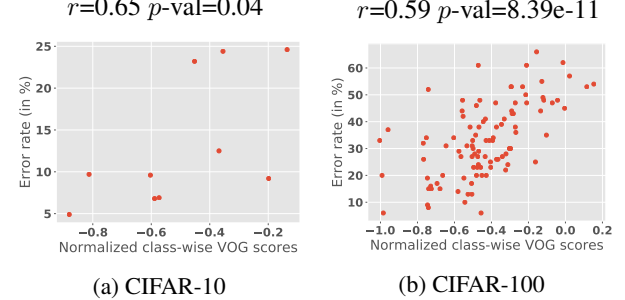


Figure 6. Plot of class false negative rate (y-axis) against average class *VOG* score for all classes (x-axis). **Left:** CIFAR-10 **Right:** CIFAR-100. There is a statistically significant positive correlation between class level error metrics and average *VOG* score (alpha set at 0.05).

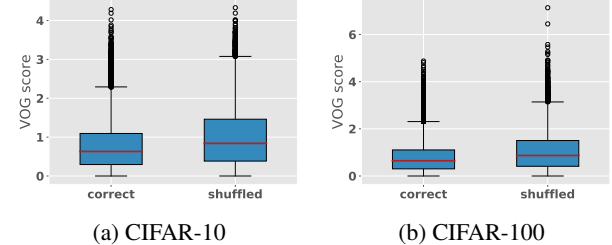


Figure 7. Box-plot of subset the *VOG* distribution of all examples with *correct* labels against the 20% of the dataset with *shuffled* labels. It is visible that the distribution of *VOG* scores, both the mean (red line in the plot) and spread, for shuffled data is higher than that of the correct samples for both CIFAR-10 (a) and CIFAR-100 (b).

4. Related Work

Our work proposes a method to rank training and test examples by estimated difficulty. Given the size of modern day datasets, this can be a powerful interpretability tool to isolate a tractable subset of examples for human-in-the-loop auditing. Prior work has proposed different notions of what subset merits surfacing. Early work by (Zhang, 1992; Bien & Tibshirani, 2012; Kim et al., 2015; Kim et al., 2016) that introduced the notion of prototypes, quintessential examples in the dataset, but did not focus on deep neural networks. Kim et al. (2016) also requires assumptions about the statistics of the input distribution. Work by Li et al. (2017) requires modifying the architecture to prefix an autoencoder

in order to surface a set of prototypes. [Koh & Liang \(2017\)](#) proposes influence functions to identify training points most influential on a given prediction.

Unlike previous works, we propose a measure that can be extended to rank the entire dataset by estimated difficulty (rather than surfacing a prototypical subset). Additionally, ranking individual samples using methods like [\(Koh & Liang, 2017\)](#) would be extremely computationally extensive. Our method does not require modifying the architecture or making any any assumptions about the statistics of the input distribution. In that sense, our work is complementary to recent work by [Jiang et al. \(2020\)](#) which proposes a c-score to rank each example by alignment with the training instances, [Hooker et al. \(2019\)](#) which classify examples as outliers according to sensitivity to varying model capacity and [Carlini et al. \(2019\)](#) which consider several different measures to isolate prototypes that could conceivably be extended to rank the entire dataset. We note that the c-score method proposed by [Jiang et al. \(2020\)](#) is considerably computationally intensive to compute than VOG as it requires training up to 20,000 network replications per data set. Several of the propotype methods considered by [Carlini et al. \(2019\)](#) require training ensembles of models, as does the compression sensitivity measure proposed by [Hooker et al. \(2019\)](#). Our method is both different in formulation and can be leveraged using a small number of existing checkpoints saved over the course of training.

5. Discussion and Future Work

Our methodology offers one way for humans to better understand the relative difficulty of different examples. One of our key findings is that VOG is far more challenging to classify for the algorithm and surfaces clusters of images with distinct visual properties. VOG is straight-forward to compute and can take advantage of current best practices of storing multiple checkpoints over the course of training. In practice, a domain expert may choose to compute VOG for a class of particular interest which would further reduce the computational cost. This is in contrast to works like [\(Li et al., 2017; Koh & Liang, 2017\)](#), which are far more computationally expensive.

Limitations and Future Work We evaluate VOG on small scale datasets such CIFAR-10 and CIFAR-100. Future questions of interest include scaling to more complex datasets. A natural extension of our research is to explore how this subset of data points can be leveraged by a human-in-the-loop domain expert to cleanup the dataset or audit potential biases. Other potential use cases include active learning and curriculum learning.

References

- Achille, A., Rovere, M., and Soatto, S. Critical learning periods in deep neural networks. *ArXiv*, abs/1711.08856, 2017.
- Badgeley, M., Zech, J., Oakden-Rayner, L., Glicksberg, B., Liu, M., Gale, W., McConnell, M., Percha, B., and Snyder, T. Deep learning predicts hip fracture using confounding patient and healthcare variables. *npj Digital Medicine*, 2:31, 04 2019. doi: 10.1038/s41746-019-0105-1.
- Baehrens, D., Schroeter, T., Harmeling, S., Kawanabe, M., Hansen, K., and MĂžller, K.-R. How to explain individual classification decisions. *Journal of Machine Learning Research*, 11(Jun):1803–1831, 2010.
- Bartlett, P. L. and Wegkamp, M. H. Classification with a reject option using a hinge loss. *J. Mach. Learn. Res.*, 9:1823–1840, June 2008. ISSN 1532-4435. URL <http://dl.acm.org/citation.cfm?id=1390681.1442792>.
- Bien, J. and Tibshirani, R. Prototype selection for interpretable classification. *arXiv e-prints*, art. arXiv:1202.5933, February 2012.
- Carlini, N., Erlingsson, Ú., and Papernot, N. Distribution Density, Tails, and Outliers in Machine Learning: Metrics and Applications. *arXiv e-prints*, art. arXiv:1910.13427, October 2019.
- Caruana, R. Case-based explanation for artificial neural nets. In Malmgren, H., Borga, M., and Niklasson, L. (eds.), *Artificial Neural Networks in Medicine and Biology*, pp. 303–308, London, 2000. Springer London. ISBN 978-1-4471-0513-8.
- Cortes, C., DeSalvo, G., and Mohri, M. Boosting with abstention. In Lee, D. D., Sugiyama, M., Luxburg, U. V., Guyon, I., and Garnett, R. (eds.), *Advances in Neural Information Processing Systems 29*, pp. 1660–1668. Curran Associates, Inc., 2016. URL <http://papers.nips.cc/paper/6336-boosting-with-abstention.pdf>.
- Dastin, J. Amazon scraps secret ai recruiting tool that showed bias against women. *Reuters*, 2018. URL <https://reut.rs/2p0ZWqe>.
- Faghri, F., Duvenaud, D., Fleet, D. J., and Ba, J. A Study of Gradient Variance in Deep Learning. *arXiv e-prints*, art. arXiv:2007.04532, July 2020.
- Feldman, V. Does learning require memorization? a short tale about a long tail. *Proceedings of the 52nd Annual ACM SIGACT Symposium on Theory of Computing*, 2020.
- Gruetzmacher, R., Gupta, A., and Paradice, D. B. 3d deep learning for detecting pulmonary nodules in ct scans. *Journal of the American Medical Informatics Association : JAMIA*, 25 10:1301–1310, 2018.
- Harwell, D. A face-scanning algorithm increasingly decides whether you deserve the job. *The Washington Post*, 2019. URL <https://wapo.st/2X3bupO>.
- He, K., Zhang, X., Ren, S., and Sun, J. Deep residual learning for image recognition. In *Proceedings of the IEEE conference on computer vision and pattern recognition*, pp. 770–778, 2016.
- Hooker, S., Courville, A., Clark, G., Dauphin, Y., and Frome, A. What Do Compressed Deep Neural Networks Forget? *arXiv e-prints*, art. arXiv:1911.05248, November 2019.
- Jiang, Z., Zhang, C., Talwar, K., and Mozer, M. C. Characterizing Structural Regularities of Labeled Data in Overparameterized Models. *arXiv e-prints*, art. arXiv:2002.03206, February 2020.
- Jiang, Z., Zhang, C., Talwar, K., and Mozer, M. C. Exploring the memorization-generalization continuum in deep learning. *arXiv preprint arXiv:2002.03206*, 2020.
- Kim, B., Rudin, C., and Shah, J. The Bayesian Case Model: A Generative Approach for Case-Based Reasoning and Prototype Classification. *arXiv e-prints*, art. arXiv:1503.01161, March 2015.
- Kim, B., Khanna, R., and Koyejo, O. O. Examples are not enough, learn to criticize! criticism for interpretability. In Lee, D. D., Sugiyama, M., Luxburg, U. V., Guyon, I., and Garnett, R. (eds.), *Advances in Neural Information Processing Systems 29*, pp. 2280–2288. Curran Associates, Inc., 2016.
- Koh, P. W. and Liang, P. Understanding Black-box Predictions via Influence Functions. *arXiv e-prints*, art. arXiv:1703.04730, March 2017.
- Krizhevsky, A., Hinton, G., et al. Learning multiple layers of features from tiny images. 2009.
- Leibig, C., Allken, V., Ayhan, M. S., Berens, P., and Wahl, S. Leveraging uncertainty information from deep neural networks for disease detection. *Scientific Reports*, 7, 12 2017. doi: 10.1038/s41598-017-17876-z.
- Li, O., Liu, H., Chen, C., and Rudin, C. Deep learning for case-based reasoning through prototypes: A neural network that explains its predictions. *CoRR*, abs/1710.04806, 2017. URL <http://arxiv.org/abs/1710.04806>.

Mangalam, K. and Prabhu, V. U. Do deep neural networks learn shallow learnable examples first. 2019.

NHTSA. Technical report, U.S. Department of Transportation, National Highway Traffic, Tesla Crash Preliminary Evaluation Report Safety Administration. *PE 16-007*, Jan 2017.

Oakden-Rayner, L., Dunnmon, J., Carneiro, G., and Ré, C. Hidden Stratification Causes Clinically Meaningful Failures in Machine Learning for Medical Imaging. *arXiv e-prints*, art. arXiv:1909.12475, Sep 2019.

Simonyan, K., Vedaldi, A., and Zisserman, A. Deep inside convolutional networks: Visualising image classification models and saliency maps. *arXiv preprint arXiv:1312.6034*, 2013.

Xie, H., Yang, D., Sun, N., Chen, Z., and Zhang, Y. Automated pulmonary nodule detection in ct images using deep convolutional neural networks. *Pattern Recognition*, 85:109 – 119, 2019. ISSN 0031-3203. doi: <https://doi.org/10.1016/j.patcog.2018.07.031>. URL <http://www.sciencedirect.com/science/article/pii/S0031320318302711>.

Zhang, C., Bengio, S., Hardt, M., Recht, B., and Vinyals, O. Understanding deep learning requires rethinking generalization. *arXiv preprint arXiv:1611.03530*, 2016.

Zhang, J. Selecting typical instances in instance-based learning. In Sleeman, D. and Edwards, P. (eds.), *Machine Learning Proceedings 1992*, pp. 470 – 479. Morgan Kaufmann, San Francisco (CA), 1992. ISBN 978-1-55860-247-2. doi: <https://doi.org/10.1016/B978-1-55860-247-2.50066-8>. URL <http://www.sciencedirect.com/science/article/pii/B9781558602472500668>.